Multi-Gbit/s optical phase chaos communications using a time-delayed optoelectronic oscillator with a three-wave interferometer nonlinearity

Jérémy Oden, Roman Lavrov, Yanne K. Chembo, and Laurent Larger

Citation: Chaos **27**, 114311 (2017); doi: 10.1063/1.5007867
View online: http://dx.doi.org/10.1063/1.5007867
View Table of Contents: http://aip.scitation.org/toc/cha/27/11
Published by the American Institute of Physics

Multi-Gbit/s optical phase chaos communications using a time-delayed optoelectronic oscillator with a three-wave interferometer nonlinearity

Jérémy Oden,[1] Roman Lavrov,[1] Yanne K. Chembo,[1,2,a)] and Laurent Larger[1]
[1]*Optics Department, CNRS, FEMTO-ST Institute, University of Bourgogne Franche-Comté, 15B Avenue des Montboucons, 25030 Besançon Cedex, France*
[2]*GeorgiaTech-CNRS Joint International Laboratory [UMI 2958], Atlanta Mirror Site, School of Electrical and Computer Engineering, 777 Atlantic Drive NW, Atlanta, Georgia 30332, USA*

(Received 15 May 2017; accepted 4 September 2017; published online 19 October 2017)

We propose a chaos communication scheme based on a chaotic optical phase carrier generated with an optoelectronic oscillator with nonlinear time-delay feedback. The system includes a dedicated non-local nonlinearity, which is a customized three-wave imbalanced interferometer. This particular feature increases the complexity of the chaotic waveform and thus the security of the transmitted information, as these interferometers are characterized by four independent parameters which are part of the secret key for the chaos encryption scheme. We first analyze the route to chaos in the system, and evidence a sequence of period doubling bifurcations from the steady-state to fully developed chaos. Then, in the chaotic regime, we study the synchronization between the emitter and the receiver, and achieve chaotic carrier cancellation with a signal-to-noise ratio up to 20 dB. We finally demonstrate error-free chaos communications at a data rate of 3 Gbit/s. *Published by AIP Publishing*. https://doi.org/10.1063/1.5007867

The purpose of optical chaos communications is to secure optical fiber networks at the physical layer level using chaotic laser carriers. This analog communication scheme is based on the synchronization of two chaotic laser beams, and security in this case is ensured at the physical layer of the broadband chaos generator architecture. The basic principle of operation is that an information-bearing signal which is encrypted within the noise-like output of a large amplitude chaotic emitter, while a synchronous receiver recognizes the deterministic chaotic component and cancels it to reveal the initially encrypted signal. Several optical chaos cryptosystems have been demonstrated so far, either based on semiconductor lasers with optical feedback or on time-delayed optoelectronic oscillators.[1,2] In this article, we propose a new architecture for optical chaos communications belonging to the latter category, and for which the key element is a customized three-wave fiber interferometer. We show that this system outputs a broadband optical phase chaos that can be accurately synchronized with negligible residual noise, and allows for successful multi-Gbit/s optical chaos communications.

I. INTRODUCTION

The pioneering work of Ikeda about 40 years ago evidenced the possibility to obtain optical chaos using a delayed system with local nonlinearity.[3–5] The proof-of-concept experiments of Neyer and Voges[6] have permitted to implement Ikeda-like systems using off-the-shelf telecom devices, and have thereby facilitated the study of many fundamental phenomena related to nonlinear time-delay dynamics in photonics (see for example Refs. 7–25). Beyond the fundamental analysis of this system as a paradigm for delayed dynamics,[26,27] numerous applications have benefited from this research, which include ultra-pure microwave generation,[28–42] photonic reservoir computing (see Refs. 43–49 and references therein), or optical chaos communications,[50–55] among others.[1,56]

In the area of optical chaos communications, Ikeda-like systems have been shown to be particularly suitable and versatile. Effectively, several architectures have been proposed with the chaotic variable being the wavelength, the intensity of the phase of the laser carrier signal.[1] The robustness of this technology has been tested in two key field experiments. In the first one, a 3 Gbit/s transmission over 120 km has been achieved in the metropolitan optical fiber network of Athens, Greece, using the optical intensity chaos[50] with 10^{-7} bit-error rate (BER). In the second experiment, a record 10 Gbit/s transmission over 22 km was achieved in the *Lumière* optical fiber network of Besançon, France, using optical phase chaos.[51] This work has also enabled to emphasize on the specific advantages of optical phase encryption with regards to conventional amplitude encryption.

In general, the nonlinear function ruling the chaotic dynamics is characterized by a single free parameter. However, it is known that the security of the transmission increases with the dimensionality for the physical cryptographic key, which is the set of free parameters ruling the encrypting chaos dynamics. Therefore, from that perspective, increasing the dimensionality of the nonlinearity strengthens the security of the cryptosystem, because chaos synchronization requires the identification and matching of additional parameters. A first result along that line was achieved in Ref. 57, where the generation of optical intensity chaos was demonstrated using an integrated four-wave optical interferometer—the so-called quadrature phase-shift-keying (QPSK) electro-optic modulator. The two independent

a)Electronic mail: yanne.chembo@femto-st.fr

electro-optic modulation inputs corresponded to a two-dimensional nonlinearity which permitted to enhanced chaos complexity over a bandwidth spanning from ~0 to 13 GHz.

Research in optical chaos cryptography has shown that record-high data rates and high security are more likely to be obtained *via* optical phase encryption schemes.[51] The corresponding emitter-receiver systems are broadband optoelectronic oscillators featuring conventional two-wave interferometers (differential phase shift keying—DPSK-demodulator) in the delayed feedback loop. However, this commercially available two-wave interferometer yields a low dimensional encryption key space for the definition of the nonlinear function required to generate chaos. In this article, we propose to extend the concept to *a priori* much higher dimensional encryption key space involving a multiple wave imbalanced interferometer, whose physical parameters are determined at the fabrication stage of customized devices. This results in a hardware-based security, without the physical availability of which the real-time decoding difficulty is expected to be strongly enhanced. The expected outcome is to increase chaos complexity, and strengthen the security of the transmitted messages. An experimental demonstration of the concept is obtained with a customized matched pair three-wave interferometer involving two different time imbalancing, and two different relative static phase shifts between the interferometer arm.

The outline of the article is as follows: in Sec. II, we will first present our custom three-wave interferometer. Then, we will present the optical phase chaos generator in Sec. III, along with the model describing its dynamics. Section IV will be devoted to the synchronization of the emitter-receiver system, and to the study of multi-Gbit/s chaos communications. Section V will conclude the article.

II. THE IMBALANCED THREE-WAVE INTERFEROMETER

Two-wave interferometers are generally used in photonics to implement nonlinear transfer functions f_{NL} for the intensity of laser beams, following $P_{out} = P_{in} f_{NL}[\alpha]$, where α is a control parameter (generally a phase shift), while $P_{in,out}$ are input and output powers, respectively.

The most widespread example is the integrated Mach–Zehnder (MZ) modulator, which is generally based on a two-wave balanced interferometer. In that case, an optical signal is split into two equal sub-signals which follow two distinct optical paths before being recombined. A voltage-dependent phase difference ϕ between both paths enables to control the output power *via* the sinusoidal modulation function $f_{NL} \equiv \cos^2(\phi)$, thereby providing a mechanism to control the output light intensity with a voltage V (time-dependent of not). Several chaos generators based on two-wave interferometers have been proposed so far using integrated MZ electro-optic modulators. As indicated earlier, broadband hyperchaos has also been demonstrated with an integrated four-wave interferometer, implemented with a quadrature phase-shift-keying (QPSK) electro-optic modulator.

On the other hand, architectures for broadband phase (instead of intensity) chaos generation have been introduced through the use of imbalanced passive two-wave interferometers, where the difference of optical paths is induced by e.g., a propagation length difference in two short patches of optical fiber. Electro-optic phase modulation is provided externally, and time imbalance in the interferometer is required here in order to dynamically and nonlinearly convert the phase modulation into strong intensity modulation, as long as the optical phase can be modulated faster than the time imbalance. So far, only two-wave interferometers have been considered in experimental implementations,[51,52] since they correspond to commercially available devices known as DPSK demodulators. In this work, we consider a customized three-wave interferometers instead, whose simplified architecture is displayed in Fig. 1. These interferometers have been custom-designed by the photonics company Kylia in matched pairs, and they are characterized by four parameters: the fixed time-delays ΔT_1 and ΔT_2 inducing the two arm imbalance with regards to a third (reference) one; and the two tunable phase shifts ϕ_1 and ϕ_2 which are controlled by local thermal tuning (heating). These three-wave interferometers can be characterized by their spectral filtering response in the Fourier domain

$$f_{NL}(\phi_1, \phi_2) = \frac{1}{16}\{3 + 2\cos[\phi_1 + 2\pi\Delta T_1\,\delta\nu] + 2\cos[\phi_2 + 2\pi\Delta T_2\,\delta\nu] + 2\cos[(\phi_1 - \phi_2) + 2\pi(\Delta T_1 - \Delta T_2)\,\delta\nu]\}, \quad (1)$$

where $\delta\nu$ is the optical frequency deviation from a reference optical frequency. In contrast with a two-wave interferometer which yields a 2D contribution to the encryption key space for the nonlinearity (controlled by a single phase shift ϕ, and a time imbalance ΔT), the nonlinear phase-to-intensity modulation transfer function of a three-wave interferometer can be considered as a 4D contribution, as there are two free control parameters ϕ_1 and ϕ_2 and two relative time imbalance ΔT_1 and ΔT_2.

The values of the imbalanced delays in our three-wave interferometer are $\Delta T_1 \simeq 180$ ps, $\Delta T_2 \simeq 300$ ps, while ϕ_1 and ϕ_2 have an accordability range of approximately 16π. The ratio between these delays is $\Delta T_1/\Delta T_2 = 3/5$, and we deduce that the free-spectral range of the interferometer is $\mathrm{FSR} = 3/\Delta T_1 = 5/\Delta T_2 = 16.67$ GHz. From the experimental viewpoint, the spectral characteristic transfer function of the interferometer can be obtained by performing a frequency scan which reveals the filtering profile ruled by the passive device. Figure 2 shows how this multiperiodic transfer function can be recovered analytically by adjusting the control parameters ϕ_1 and ϕ_2. The very good agreement

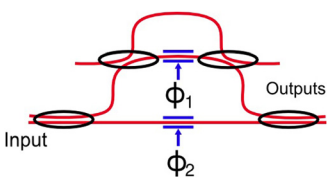

FIG. 1. Simplified equivalent model for the three-wave interferometer. The double-digit labels identify the possible input/output ports. The static phases ϕ_1 and ϕ_2 can be tuned using a controlled thermal heating system.

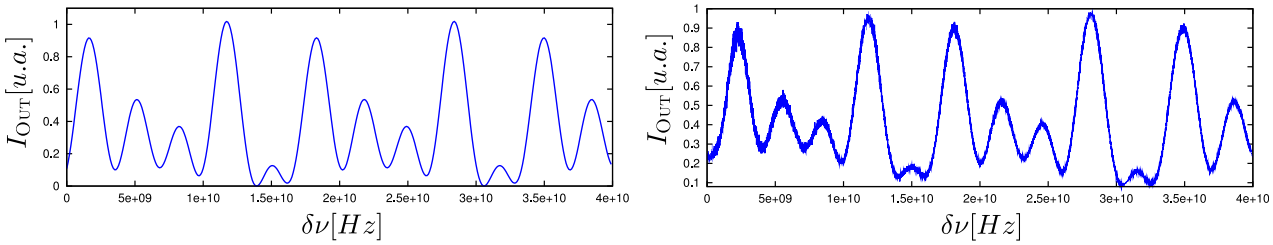

FIG. 2. Multi-periodic transfer function of the three-wave interferometer, as a function of the detuning frequency $\delta\nu$. The tunable (free) parameters are ϕ_1 and ϕ_2. Left: theoretical curve adjusted to measurements; right: experimental curve.

between experimental and theoretical results indicates that the characteristic features of the three-wave imbalanced interferometers are well controlled and can be tuned with a high degree of precision (of the order of 1%), which is a prerequisite to obtain synchronized chaotic phase dynamics. It is worth mentioning here that the multiple wave interferometer is characterized as a linear optical filter for the electromagnetic field amplitude, it is however involved as a nonlinear dynamical element considering the optical phase modulation as an input signal of this filter, and the light intensity (averaged by a photodiode) output of the filter.

III. THE OPTICAL PHASE CHAOS OSCILLATOR

Optical phase chaos is generated using a broadband optoelectronic oscillator (Fig. 3). In this oscillator, a continuous-wave (CW) laser with wavelength around 1550 nm and phase Φ_0 seeds a phase modulator for the message encryption, which outputs an optical laser beam with a modulated phase $\Phi_M(t)$. The phase modulated laser beam is fed into a second phase modulator which outputs an optical signal with phase $\Phi_T(t)$. A 50/50 coupler permits to extract a half of the signal to an output port, while the second half is launched into a delay line of length $L = v_g T$, where T is the time-delay and v_g is the group velocity in the optical fiber. The delayed optical signal is then inserted in a three-wave interferometer, which performs a nonlinear phase-to-intensity transformation and acts like a nonlocal nonlinearity in time (due to the two time imbalance). The output optical intensity signal is detected by a fast photodiode to result in an electrical signal, which is amplified, and connected back to the radio-frequency (RF) input of the second phase modulator to close the feedback loop. Overall, the signal in the feedback loop, therefore undergoes three slightly different delays, namely T, $T + \Delta T_1$ and $T + \Delta T_2$ and some of their differences through the interference process.

The optoelectronic elements of the loop (in particular the RF amplifier and the photodiode) are frequency-selective, and as a consequence the feedback loop features band-pass filtering properties. The RF amplifier (DR-DG-20-HO) has a gain of 32 dB and a bandwidth ranging from ∼100 kHz to ∼23 GHz, and the photodiodes have a bandwidth >10 GHz. However, the low-pass filtering is performed in the feedback loops by introducing low-pass filters with a cut-off frequency of 7.73 GHz. For the sake of simplicity, one can consider that this band-pass filter corresponds to cascaded first-order high-pass and low-pass filters of cut-off frequencies f_H and f_L, respectively. The variable of interest in this dynamical system is the phase $\Phi(t)$ of the optical field at the input of the phase modulator PM_M. This variable is transduced to an optical intensity by the three-wave fiber interferometer, and subsequently, to an electrical fluctuation after fast photodetection. It can be demonstrated that the variable $x(t) = \Phi(t)/2$ obeys the following multiple delay integro-differential equation

$$x + \tau \frac{dx}{dt} + \frac{1}{\theta}\int_{t_0}^{t} x(\xi)\, d\xi = \beta\, \mathrm{F_{NL}}\{x_T, x_{T+\Delta T_1}, x_{T+\Delta T_2}\}, \quad (2)$$

where β is the normalized feedback loop gain, $\tau = 1/2\pi f_L$ and $\theta = 1/2\pi f_H$ correspond to the low- and high-pass filters cut-off times, respectively, while

$$\begin{aligned}\mathrm{F_{NL}}\{x_T, x_{T+\Delta T_1}, x_{T+\Delta T_2}\} &= \frac{1}{9}\{3 + 2\cos[x_T - x_{T+\Delta T_1} + \phi_1] \\ &+ 2\cos[x_T - x_{T+\Delta T_2} + \phi_2] \\ &+ 2\cos[x_{T+\Delta T_1} - x_{T+\Delta T_2} + (\phi_1 - \phi_2)]\} \end{aligned} \quad (3)$$

with $x_T \equiv x(t - T)$ by definition.

The dynamics of this system can be understood from the numerical bifurcation diagram of Fig. 4. Indeed, below a

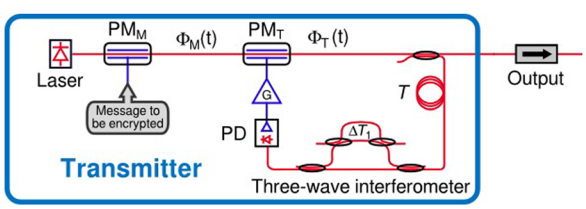

FIG. 3. Architecture of the optical phase chaos generator. PM: phase modulator and PD: photodiode.

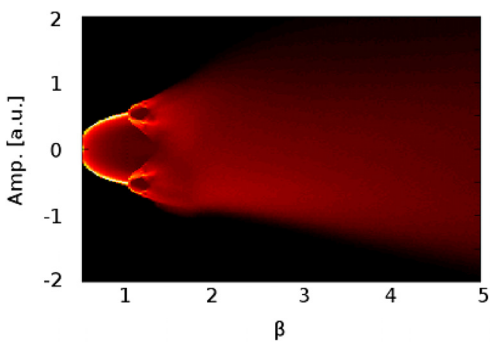

FIG. 4. Numerical bifurcation diagram, obtained after the numerical simulation of Eq. (2). It evidences a period-doubling route to chaos.

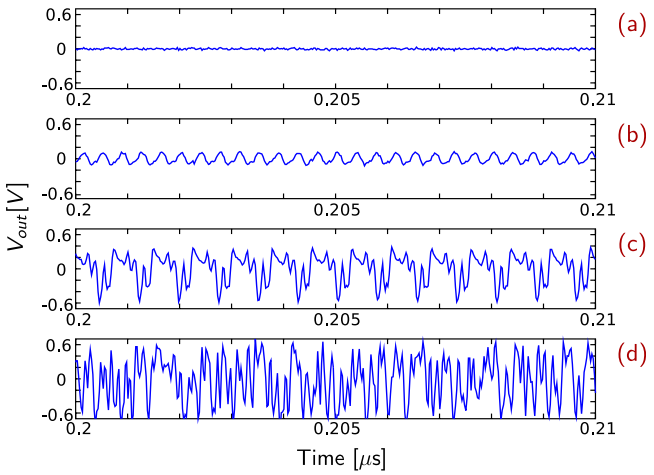

FIG. 5. Experimental timetraces for the optical phase chaos generator. (a) $P_{in} = 4.5$ dBm: stationary regime; (b) $P_{in} = 5.4$ dBm: periodic regime; (c) $P_{in} = 7.1$ dBm: multiperiodic regime; and (d) $P_{in} = 9.0$ dBm: chaotic regime.

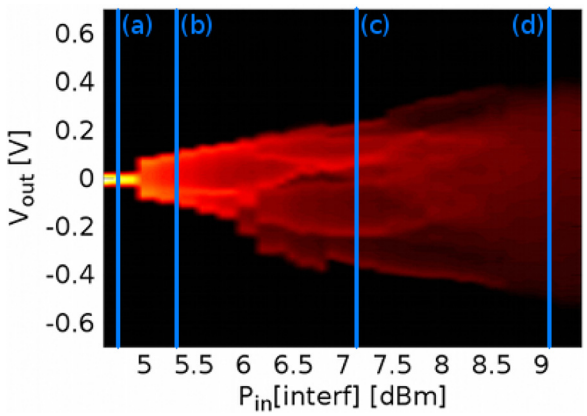

FIG. 6. Experimental bifurcation diagram showing the route to chaos. The vertical lines (a)–(d) correspond to the timetraces of Fig. 5.

certain critical bifurcation value β_{cr}, the system remains at the trivial fixed point $x_0 \equiv 0$. Then, as the system is driven beyond β_{cr}, a first Hopf bifurcation leads the system to a limit-cycle. Further increase of β leads to a sequence of period-doubling bifurcations, and ultimately, to fully developed hyperchaos, a regime of obvious interest for our chaos communication purpose.

Our experimental measurements confirm this scenario, and unveil the rich dynamical nature of this time-delayed system as well. In Fig. 5, the experimental timetraces obtained for various values of the laser pump power P_{in} are displayed. Since the parameter β is proportional to P_{in}, this is equivalent to exploring the dynamics of the system for different values of the feedback gain. It can be observed that as the gain is increased, the system is first in the trivial

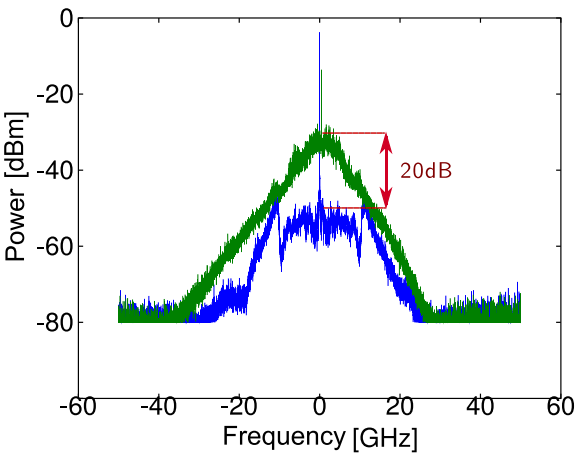

FIG. 8. Experimental spectra of the chaotic carrier (green) and synchronization error (blue) signals. Chaos cancellation ranges from 15 to 20 dB in a 10 GHz bandwidth around the optical carrier.

stationary state, and then bifurcates to periodic, multiperiodic, and finally chaotic states. This behavior is recovered when P_{in} is scanned continuously, thereby leading to the experimental bifurcation diagram of Fig. 6. We note that this experimental bifurcation diagram actually appears more complex than the numerical one. This is an indication that the complexity of the experimental system is higher than the one predicted by the model.

IV. SYNCHRONIZATION AND OPTICAL CHAOS COMMUNICATIONS

Chaos communications rely on synchronization: therefore, a receiver matching the emitter architecture has to be implemented in order to retrieve successfully the chaotic carrier, the latter being subtracted from the received encoded signal to retrieve the initial clear information. As shown in Fig. 7, our receiver is identical to the emitter, with three key differences. First, the receiver has an open-loop architecture, as the output of the phase modulator is injected into the three-wave interferometer. Second, the amplifier is also an inverting one, so that the chaotic modulation is anti-synchronized to the one of the emitter; this feature enables us to cancel out the chaotic part of the incoming phase modulated optical signal, as required by chaos communication protocols. Finally, the optical output (with a canceled chaotic carrier) is connected to a differential-phase shift keying (DPSK) demodulator and to a fast photodetector in order to recover in the electrical domain the resulting phase demodulated information. In the absence of any phase information modulation (message free transmission), the output of the photodetector is a residual noise referred to as *synchronization error*.

The physical parameters characterizing the emitter and receiver (photodiodes, three-wave interferometers, RF

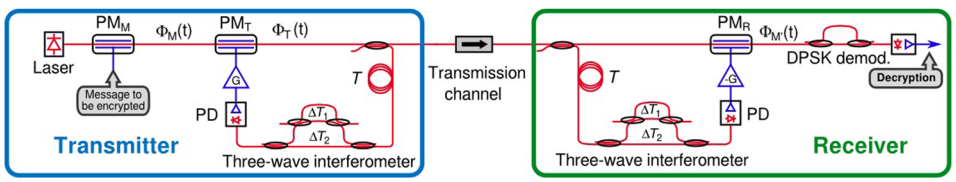

FIG. 7. Architecture of the emitter-receiver system for optical phase chaos communications.

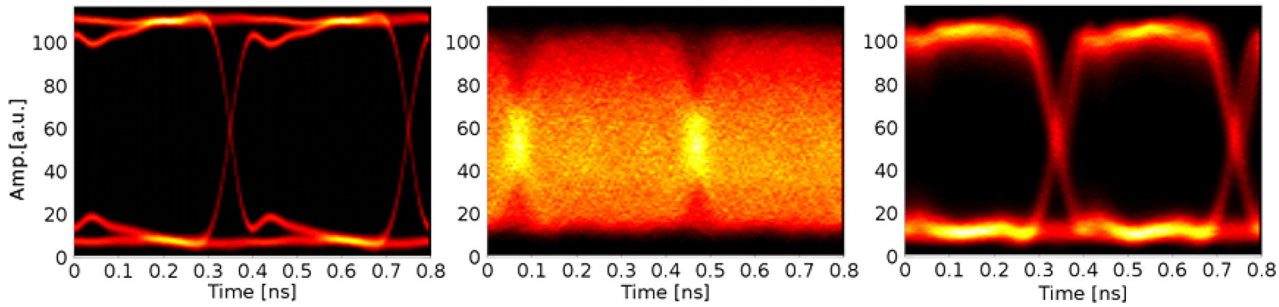

FIG. 9. Experimental eye diagram for a back-to-back configuration. Left: eye diagram of the transmitted message at 3 Gbit/s; center: eye diagram of the encrypted message; right: eye diagram of the decrypted message, with a BER below 10^{-12}.

amplifiers, phase modulators, etc.) are ideally expected to be identical. In that case, synchronization is perfect and the synchronization error is exactly null.[58–60] However, there are unavoidable sources of noise and parameter mismatch between the emitter and receiver, resulting in a synchronization error.[7,61,62] The free parameters of the system are τ, θ, β, T, ΔT_1, ΔT_2, ϕ_1 and ϕ_2. In our experimental system, they are matched within 1% accuracy. In particular, the photonics company Kylia has provided us a matched pair of two three-wave interferometers with intrinsic parameters ΔT_1 and ΔT_2 finely adjusted within 0.1%. Figure 8 shows the spectra of both the chaotic carrier and the synchronization error. It can be seen that chaos cancellation is achieved with a performance ranging from 15 to 20 dB, over a spectral range of 20 GHz around the carrier.

Broadband chaos cancellation indicates that chaos communications can be performed at high rate with a satisfying BER. The value of the normalized feedback gain was fixed to $\beta = 3$ and we have matched the values of the phase offsets ϕ_1 and ϕ_2 for both interferometers. Indeed, as shown in Fig. 9, we have successfully achieved encryption and decryption of binary data at 3 Gbit/s, with a bit-error rate better than 10^{-12} (the error detection threshold of our equipment).

V. CONCLUSION

In this article, we have presented a broadband optoelectronic oscillator which outputs optical phase chaos. We have studied the bifurcation structure of this oscillator, and investigated as well an emitter-receiver architecture for chaos synchronization. The good chaos cancellation ratio permits to perform error-free chaos communications at a data rate of 3 Gbits/s. Our results have demonstrated the efficiency of optical phase chaos communication approaches, and their implementation through customized devices offering a hardware encryption key.

Future research will be devoted to the optimization of this communication scheme, and to a deeper understanding of the nonlinear dynamics of the chaos generator. The three-wave interferometer device has been operated without the need for any active control of the different internal parameters (offset phase differences, essentially), contrarily to the previous experiments on phase chaos generation and synchronization which have used the fiber-based two-wave interferometer. Our three-wave interferometer was indeed designed with free space interferometer arms, thus providing negligible drifts in the internal optical paths. When considering waveguide structures which brings with it the potential for photonic chip device,[63] micro-nano-fabrication (e.g., Silicon photonic devices), one might however require to address high-dimensional control of the various internal optical paths. This represents an interesting control challenge, making use of the backward propagation as already done for the imbalanced two-wave interferometer setup.

ACKNOWLEDGMENTS

This work has been supported by the *Région de Franche-Comté* through the project CORPS, and by the LabEx ACTION.

[1]L. Larger, Philos. Trans. R. Soc. A **371**, 20120464 (2013).
[2]M. C. Soriano, J. Garcia-Ojalvo, C. R. Mirasso, and I. Fischer, Rev. Mod. Phys. **85**, 421–470 (2013).
[3]K. Ikeda, Opt. Commun. **30**, 257–261 (1979).
[4]K. Ikeda, H. Daido, and O. Akimoto, Phys. Rev. Lett. **45**, 709 (1980).
[5]K. Ikeda and M. Matsumoto, J. Stat. Phys. **44**, 955–983 (1986).
[6]A. Neyer and E. Voges, IEEE J. Quantum Electron. **18**, 2009–2015 (1982).
[7]Y. C. Kouomou, P. Colet, N. Gastaud, and L. Larger, Phys. Rev. E **69**, 056226 (2004).
[8]K. E. Callan, L. Illing, Z. Gao, D. J. Gauthier, and E. Scholl, Phys. Rev. Lett. **104**, 113901 (2010).
[9]D. P. Rosin, K. E. Callan, D. J. Gauthier, and E. Scholl, Eur. Phys. Lett. **96**, 34001 (2011).
[10]L. Weicker, T. Erneux, M. Jacquot, Y. Chembo, and L. Larger, Phys. Rev. E **85**, 026206 (2012).
[11]L. Weicker, T. Erneux, O. D'Huys, J. Danckaert, M. Jacquot, Y. Chembo, and L. Larger, Phys. Rev. E **86**, 055201 (2012).
[12]C. R. S. Williams, T. E. Murphy, R. Roy, F. Sorrentino, T. Dahms, and E. Schöll, Phys. Rev. Lett. **110**, 064104 (2013).
[13]L. Weicker, T. Erneux, O. D'Huys, J. Danckaert, M. Jacquot, Y. K. Chembo, and L. Larger, Philos. Trans. R. Soc. A **371**, 20120459 (2013).
[14]B. Romeira, F. Kong, W. Li, J. M. L. Figueiredo, J. Javaloyes, and J. Yao, IEEE J. Lightwave Technol. **32**, 3933 (2014).
[15]J. Martinez-Llinas, P. Colet, and T. Erneux, Phys. Rev. E **89**, 042908 (2014).
[16]L. Weicker, T. Erneux, D. P. Rosin, and D. J. Gauthier, Phys. Rev. E **91**, 012910 (2015).
[17]J. Martinez-Llinas and P. Colet, Opt. Express **23**, 24785 (2015).
[18]W. Y. Wang, W. Li, W. H. Sun, W. Wang, J. G. Liu, and N. H. Zhu, IEEE Photonics Technol. Lett. **27**, 522 (2015).
[19]A. F. Talla *et al.*, IEEE J. Quantum Electron. **51**, 5000108 (2015).
[20]J. H. Talla Mbe *et al.*, Phys. Rev. E **91**, 012902 (2015).
[21]A. M. Hagerstrom, T. E. Murphy, and R. Roy, Proc. Natl. Acad. Sci. **112**, 9258 (2015).
[22]G. R. G. Chengui, P. Woafo, and Y. K. Chembo, IEEE J. Lightwave Technol. **34**, 873 (2016).
[23]X. Jiang, M. Cheng, F. Luo, L. Deng, S. Fu, C. Ke, M. Zhang, M. Tang, P. Shum, and D. Liu, Opt. Express **24**, 28804 (2016).

[24]Y. K. Chembo, M. Jacquot, J. M. Dudley, and L. Larger, Phys. Rev. A **94**, 023847 (2016).
[25]A. F. Talla, R. Martinenghi, P. Woafo, and Y. K. Chembo, IEEE Photonics J. **8**, 7803608 (2016).
[26]T. Erneux, *Applied Delay Differential Equations* (Springer, 2010).
[27]M. Lakshmanan and D. V. Senthilkumar, *Dynamics of Nonlinear Time-Delay Systems* (Springer, 2011).
[28]X. S. Yao and L. Maleki, Electron. Lett. **30**, 1525–1526 (1994).
[29]X. S. Yao and L. Maleki, J. Opt. Soc. Am. B **13**, 1725 (1996).
[30]X. S. Yao and L. Maleki, IEEE J. Quantum Electron. **32**, 1141 (1996).
[31]J. Yang, Y. Jin-Long, W. Yao-Tian, Z. Li-Tai, and Y. En-Ze, IEEE Photonics Technol. Lett. **19**, 807 (2007).
[32]Y. K. Chembo, L. Larger, R. Bendoula, and P. Colet, Opt. Express **16**, 9067 (2008).
[33]Y. K. Chembo, A. Hmima, P.-A. Lacourt, L. Larger, and J. M. Dudley, IEEE J. Lightwave Technol. **27**, 5160 (2009).
[34]E. C. Levy, O. Okusaga, M. Horowitz, C. R. Menyuk, W. Zhou, and G. M. Carter, Opt. Express **18**, 21461 (2010).
[35]I. Ozdur, M. Akbulut, N. Hoghooghi, D. Mandridis, M. U. Piracha, and P. J. Delfyett, Opt. Lett. **35**, 799 (2010).
[36]J. M. Kim and D. Cho, Opt. Express **18**, 14905 (2010).
[37]W. Li and J. Yao, IEEE J. Lightwave Technol. **28**, 2640 (2010).
[38]L. Maleki, Nat. Photonics **5**, 728 (2011).
[39]R. M. Nguimdo, Y. K. Chembo, P. Colet, and L. Larger, IEEE J. Quantum Electron. **48**, 1415–1423 (2012).
[40]K. Saleh *et al.*, Opt. Express **22**, 32158 (2014).
[41]S. Jia *et al.*, IEEE Photonics Technol. Lett. **27**, 213 (2014).
[42]Y. Zhang, D. Hou, and J. Zhao, J. Lightwave Technol. **32**, 2408 (2014).
[43]L. Appeltant *et al.*, Nat. Commun. **2**, 468 (2011).
[44]Y. Paquot, F. Duport, A. Smerieri, J. Dambre, B. Schrauwen, M. Haelterman, and S. Massar, Sci. Rep. **2**, 287 (2012).
[45]D. Brunner, M. C. Soriano, C. R. Mirasso, and I. Fischer, Nat. Commun. **4**, 1364 (2013).
[46]M. C. Soriano *et al.*, Opt. Express **21**, 12 (2013).
[47]F. Duport, A. Smerieri, A. Akrout, M. Haelterman, and S. Massar, Sci. Rep. **6**, 22381 (2016).
[48]G. Van der Sande, D. Brunner, and M. C. Soriano, Nanophotonics **6**, 561 (2017).
[49]L. Larger *et al.*, Phys. Rev. X **7**, 011015 (2017).
[50]A. Argyris, D. Syvridis, L. Larger, V. Annovazzi-Lodi, P. Colet, I. Fischer, J. Garcia-Ojalvo, C. R. Mirasso, L. Pesquera, and K. A. Shore, Nature **438**, 343–346 (2005).
[51]R. Lavrov, M. Jacquot, and L. Larger, IEEE J. Quantum Electron. **46**, 1430 (2010).
[52]R. M. Nguimdo, R. Lavrov, P. Colet, M. Jacquot, Y. K. Chembo, and L. Larger, IEEE J. Lightwave Technol. **28**, 2688 (2010).
[53]A. Uchida, *Optical Communication with Chaotic Lasers: Applications of Nonlinear Dynamics and Synchronization Wiley* (Wiley, 2012).
[54]R. M. Nguimdo and P. Colet, Opt. Express **20**, 25333 (2012).
[55]M. Cheng, L. Deng, H. Li, and D. Liu, Opt. Express **22**, 5241 (2014).
[56]X. Zou, X. Liu, W. Li, P. Li, W. Pan, L. Yan, and L. Shao, IEEE J. Quantum Electron. **52**, 0601116 (2016).
[57]M. Nourine, Y. K. Chembo, and L. Larger, Opt. Lett. **36**, 2833 (2011).
[58]Y. C. Kouomou and P. Woafo, Phys. Lett. A **298**, 18 (2002).
[59]Y. C. Kouomou and P. Woafo, Opt. Comm. **223**, 283 (2003).
[60]Y. C. Kouomou and P. Woafo, Phys. Rev. E **67**, 046205 (2003).
[61]A. B. Cohen, B. Ravoori, T. E. Murphy, and R. Roy, Phys. Rev. Lett. **101**, 154102 (2008).
[62]B. Ravoori, A. B. Cohen, J. Sun, A. E. Motter, T. E. Murphy, and R. Roy, Phys. Rev. Lett. **107**, 034102 (2011).
[63]A. Argyris, M. Hamacher, K. E. Chlouverakis, A. Bogris, and D. Syvridis, Phys. Rev. Lett. **100**, 194101 (2008).